Finite element simulation of cement-bone interface micromechanics; a comparison to experimental results

Dennis Janssen[1,2], Kenneth A. Mann[2], Nico Verdonschot[1]

1. Orthopaedic Research Laboratory, Radboud University Nijmegen Medical Centre, Nijmegen, The Netherlands
2. SUNY Upstate Medical University, Syracuse, NY, USA.

Abstract

Recently, experiments have been performed to determine the micromechanical behavior of the cement-bone interface. In the current study, an attempt was made to simulate these experiments using FEA. Cement-bone interface models were created of experimental specimens, based upon μCT scans. Similar to what was found experimentally, the majority of the deformation took place at the cement-bone interface. Furthermore, the simulated interface was stiffer in compression than in tension. There was a weak correlation between the predicted stiffness and the stiffness found experimentally, most likely due to the relatively high coarseness of the FEA models.

Introduction

Finite element analysis (FEA) is a valuable tool for investigation of total hip arthroplasty. One of the main advantages of FEA is the ability to isolate clinical variables and study their effect on the mechanical behavior of reconstructions in a clean, controlled manner. In the past, FEA has been used to analyze various aspects of total hip arthroplasty, such as implant migration (Huiskes *et al.*, 1998), the effect of implant design and implant material on long-term mechanical survival (Stolk *et al.*, 2007; Janssen *et al.*, 2005) and debonding of the implant-cement interface (Verdonschot and Huiskes, 1997; Perez *et al.*, 2006).

The reliability of FEA studies depends on the accuracy of the experimental and clinical data that is used as input for the models. Although much data is already available on the properties of implants, bone cement (Lewis, 1997; Murphy and Prendergast, 2002), the implant-cement interface (Davies and Harris, 1993; Mann *et al.*, 1991) and bone (Kaneko *et al.*, 2003, 2004; Taddei *et al.*, 2004), surprisingly little is known about the cement-bone interface.

The cement-bone interface consists of complex structures of cement penetrating into bone lacunar spaces, creating an interlock between bulk cement and bone. The interface provides the fixation of the cement mantle in the femur. Hence, the stability of the cement mantle and the implant is dependent on the mechanical behavior of the cement-bone interface.

Recently, experiments have been performed to determine the micromechanical behavior of the cement-bone interface (Mann *et al.*, in press). Small laboratory cement-bone interface specimens were cyclically loaded in fully reversible tension-compression, while monitoring the micromotion of the cement, bone and the cement-bone interface. The results showed that the majority of the displacement response localized at the interface between the cement and the bone. It was furthermore shown that the cement-bone interface had a relatively low stiffness compared to that of the adjacent bone and cement, and that the interface was more compliant in tension than in compression.

The goal of the present study was to simulate the bone-cement interface experiments using FEA. For this purpose, FEA models were created of the actual experimental specimens, based upon μCT scans. We investigated if micromechanical FEA structural models with frictional interfaces between the cement and bone could reproduce the low stiffness features found at the contact interface in the experiments.

Materials and methods

Experimental protocol

Cement-bone interface specimens were prepared from cemented total hip arthroplasties in fresh-frozen proximal femurs (Mann *et al.*, in press). Following cement cure, transverse sections of the reconstructions were made, which were sectioned further to prepare cement-bone composite sections with a nominal cross-section 5 x 10 mm. The specimens were then scanned at a resolution of 12 x 12 x 12 μm (Scanco μCT 40, Scanco Medical AG, Basserdorf, Switzerland).

During the experiments, the specimens were placed in an environmental chamber at 37 °C, which was filled with circulating calcium buffered saline. The models were loaded for 10 cycles of fully reversible tension and compression, with a displacement amplitude of ± 10 μm. At the tenth cycle, the reaction force and local displacements were measured. The local displacements were measured using digital image correlation techniques, in order to determine the deformation of the bone, cement and the cement-bone interface separately.

Using the force-displacement curves, the relative motion of the bone, cement and cement-bone interface were established, as well as the stiffness of the cement-bone interface in tension and compression. We furthermore measured the span of the force-displacement curves, as a measure for hysteresis occurring during one loading cycle (Figure 1).

FEA simulations

Based upon the μCT data (Figure 2a), FEA models of the experimental specimens were created using Mimics image processing and solid modeling software (Mimics 11.1, Materialise, Leuven, Belgium). The μCT data was segmented into cement and bone based upon the image grayscale. After a Boolean operation between cement and bone to prevent initial mesh penetration, a one-pixel erosion operation was performed on the cement to prevent mesh penetration at a later stage, during the subsequent remeshing procedure. From the 3D voxel meshes of the cement and bone triangular surface meshes were created. Prior to this, a 6 x 6 x 6 μCT voxel reduction was applied to limit the number of elements. This entailed that triangular surface meshing was based upon a reduced set of μCT data, introducing a geometrical error. The triangular meshes were remeshed to further limit the number of triangular elements. The triangular meshes were then exported for solid modeling. The solid models of the cement and bone were created using Patran (Patran 2005r2, MSC Software Corporation, Santa Ana, CA, USA). The resulting models (cement + bone) consisted on average of 300,000 tetrahedral elements and 71,000 nodal points (Figure 2b).

Using Mimics, material properties were assigned to the solid FEA model of the bone based upon μCT grayscale. The Young's modulus of the bone varied from virtually zero to 20.0 GPa, while a Poisson's ratio of 0.3 was assumed. The cement was assumed to have constant material properties ($E = 3.0$ GPa, $\nu = 0.3$).

Contact between the cement and bone was modeled using a node-to-surface contact algorithm (MSC.Marc2007, MSC Software Corporation, Santa Ana, CA, USA). Contact between the cement and bone was assumed to be debonded from the start of the simulation, meaning that tensile loads could only be transferred over the interface by means of an interlock of the cement and bone, rather then by a gluing capacity of the cement. Friction at the interface was modeled using a bilinear Coulomb friction model, with a friction coefficient of 0.3.

The models were loaded for a cycle of fully reversible tension and compression, mimicking the experimental protocol. During the simulation, the distal end of the cement was fixed in all directions, while the proximal end of the bone was displaced in the longitudinal direction. The proximal end of the bone was furthermore fixed such that tilting was restricted, while displacement in the transversal directions was allowed. The proximal end of the bone was displaced with incremental steps of 1.0 μm until the maximal levels of tension and compression measured during the experiment were reached.

From the force-displacement curves, again the relative motion of the bone, cement and cement-bone interface were established, as well as the stiffness of the cement-bone interface in tension and compression, and the span of the curves.

Results

The curves predicted by the FEA simulations were similar to those found experimentally (Figure 3). In most cases there was an initial deformation offset between the experimental and computational curves, most likely caused by running-in phenomena during the first nine cycles of experimental loading.

The experimental results showed that both in tension and compression more than 80 percent of the deformation took place at the cement-bone interface (Table 1). Furthermore, the bone deformed slightly more than the cement. Similar to the experiments, the FEA simulations showed that the majority of the motion took place at the cement-bone interface (Table 1). In the simulations, the cement deformed slightly more than the bone.

The predicted FEA stiffness of the interface in compression was higher than in tension, consistent with the experimental findings (Table 2). There was a weak correlation between the stiffness in tension and compression predicted by the FEA simulations and the experimental stiffness (rsq = 0.61, Figure 4). The average error between the analytical and experimental stiffness was 6.98 MPa/mm and 71.43 MPa/mm in tension and compression, respectively.

The span predicted by the FEA simulations, caused by frictional phenomena at the cement-bone interface, was lower than the span found experimentally (Table 2).

Discussion

In the present study, we investigated if micromechanical FEA structural models with frictional interfaces between the cement and bone could reproduce the low stiffness features found at the contact interface in the experiments.

The results of the FEA simulations showed that the majority of the deformation took place at the interface between the cement and bone, similar to what was found experimentally. We furthermore found that the cement-bone interface was stiffer in compression than in tension, which was also shown by the experimental results. There remains, however, room for improvement of the correspondence of the simulated and experimental stiffness values. Furthermore, the models were unable to fully capture the amount of hysteresis found experimentally.

The weak stiffness correlation and the underestimation of the hysteresis is most likely caused by the coarseness of the FEA models of the bone-cement interface specimens. The models were created from µCT-scans with a 12 x 12 x 12 µm resolution. Furthermore, the µCT-data was coarsened by a 6 x 6 x 6 voxel reduction in Mimics, after which the models were remeshed to further limit the number of elements. Considering the displacements applied to the bone-cement specimens (± 10 µm), the resulting models may very well have been too coarse to fully capture the micromechanical response displayed in the experiments. An obvious solution would therefore be to use µCT-data with a higher resolution, and to refrain from µCT-data reduction and further remeshing. This would, however, lead to model sizes of several millions of elements. Considering the non-linear nature of a node-to-surface contact analysis as used in the current study, this would result in excessive computational costs.

Despite the limitations of the current models, we were able to reproduce the micromechanical response of the cement-bone interface, using only a frictional contact at the interface. This suggests that the cement-bone interface should be regarded as mechanically unbonded. It therefore seems that the bond between cement and bone is purely generated by the interlock rather than by a gluing capacity of bone cement to bone. This emphasizes the importance of obtaining a good mechanical cement-bone interlock during total joint surgery, for instance by using pulse lavage of the intramedullary canal prior to implantation and pressurization of the cement after stem insertion.

References

Davies,J.P. and Harris,W.H. (1993) Strength of cement-metal interfaces in fatigue: comparison of smooth, porous and precoated specimens. *Clin.Mater.* **12,** 121-126.

Huiskes,R., Verdonschot,N., and Nivbrant,B. (1998) Migration, stem shape, and surface finish in cemented total hip arthroplasty. *Clin.Orthop.Relat Res.* 103-112.

Janssen,D., Aquarius,R., Stolk,J., and Verdonschot,N. (2005) Finite-element analysis of failure of the Capital Hip designs. *J.Bone Joint Surg.Br.* **87,** 1561-1567.

Kaneko,T.S., Bell,J.S., Pejcic,M.R., Tehranzadeh,J., and Keyak,J.H. (2004) Mechanical properties, density and quantitative CT scan data of trabecular bone with and without metastases. *J.Biomech.* **37,** 523-530.

Kaneko,T.S., Pejcic,M.R., Tehranzadeh,J., and Keyak,J.H. (2003) Relationships between material properties and CT scan data of cortical bone with and without metastatic lesions. *Med.Eng Phys.* **25,** 445-454.

Lewis,G. (1997) Properties of acrylic bone cement: state of the art review. *J.Biomed.Mater.Res.* **38,** 155-182.

Mann,K.A., Bartel,D.L., Wright,T.M., and Ingraffea,A.R. (1991) Mechanical characteristics of the stem-cement interface. *J.Orthop.Res.* **9,** 798-808.

Mann,K.A., Miller,M.A., Cleary,R.J., Janssen,D., Verdonschot,N. (in press) Experimental micromechanics of the cement-bone interface. *J.Orthop.Res.*

Murphy,B.P. and Prendergast,P.J. (2002) The relationship between stress, porosity, and nonlinear damage accumulation in acrylic bone cement. *J.Biomed.Mater.Res.* **59,** 646-654.

Perez,M.A., Garcia-Aznar,J.M., Doblare,M., Seral,B., and Seral,F. (2006) A comparative FEA of the debonding process in different concepts of cemented hip implants. *Med.Eng Phys.* **28,** 525-533.

Stolk,J., Janssen,D., Huiskes,R., and Verdonschot,N. (2007) Finite element-based preclinical testing of cemented total hip implants. *Clin.Orthop.Relat Res.* **456,** 138-147.

Taddei,F., Pancanti,A., and Viceconti,M. (2004) An improved method for the automatic mapping of computed tomography numbers onto finite element models. *Med.Eng Phys.* **26,** 61-69.

Verdonschot,N. and Huiskes,R. (1997) Cement debonding process of total hip arthroplasty stems. *Clin.Orthop.Relat Res.* 297-307.

Acknowledgements

This work was funded by NIH-NIAMS AR42017.

Figures

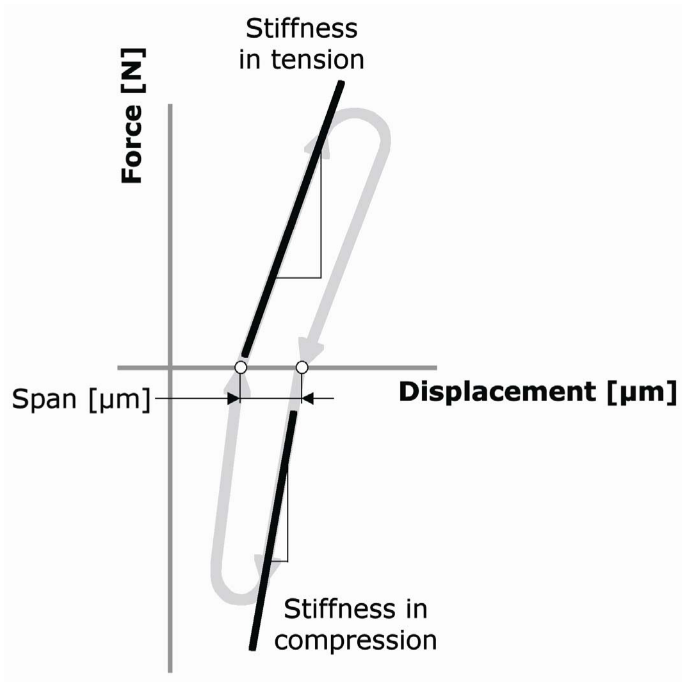

Figure 1 *Schematic force-displacement diagram with the outcome measures used in the current study.*

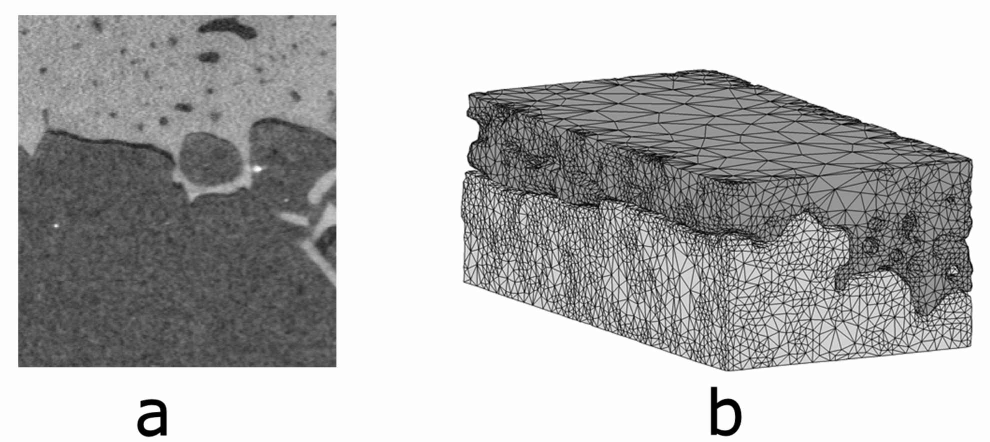

Figure 2 a) *μCT slice and b) an FEA model of a cement-bone interface specimen.*

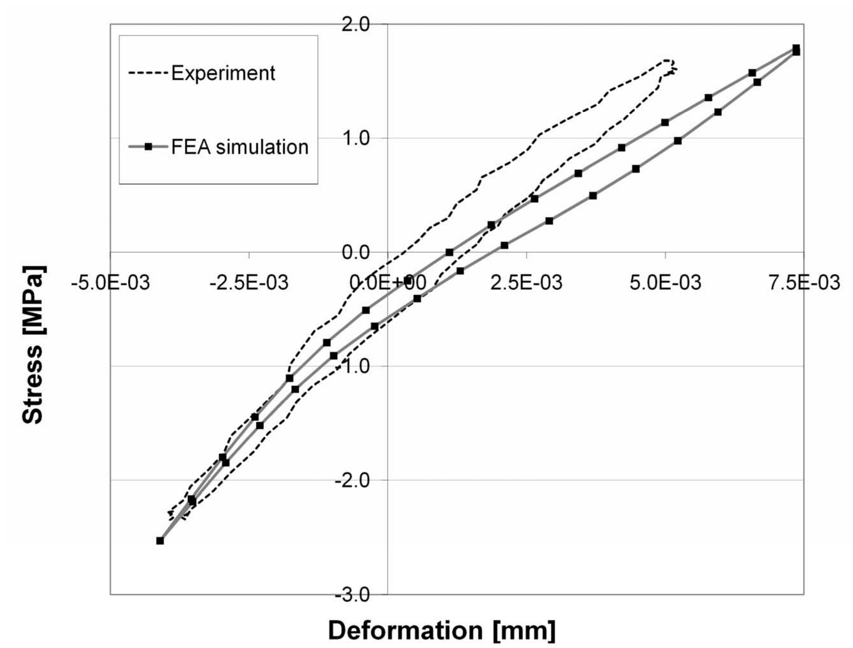

Figure 3 *Experimental and analytical force-displacement of a single specimen.*

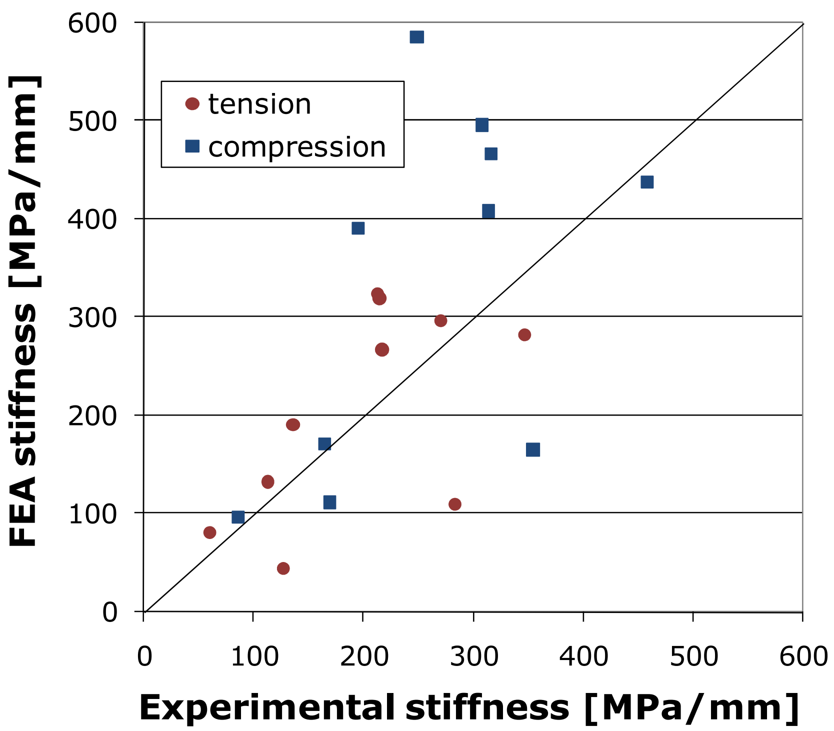

Figure 4 *Experimental versus analytical stiffness in tension and compression.*

Tables

Table 1 Relative deformation of the bone, interface and cement in percentage of the total deformation (standard deviation)

	Tension			Compression		
	bone	interface	cement	bone	interface	cement
Experiments	8.0 (9.2)	88.8 (8.7)	3.2 (5.7)	9.3 (9.1)	87.3 (10.3)	3.4 (3.5)
FEA	2.6 (2.8)	88.2 (12.2)	9.2 (11.9)	4.8 (4.6)	81.9 (14.9)	13.4 (14.3)

Table 2 Experimental and analytical compression/tension stiffness ratio of the interface, and the span of the force-displacement curves.

	Compression/tension stiffness ratio [-] (S.D.)	**Span [µm] (S.D.)**
Experiments	1.35 (0.12)	2.52 (1.36)
FEA	1.66 (0.39)	1.66 (1.44)